Facilitating Multiple Beam Production by Clustering Scattered Positrons with a Uniform Magnetic Field

Albert Farah

Abstract

Recent technologies in advanced space propulsion employ the energy of matter-antimatter annihilation, specifically between electrons and positrons, to excite D-D fusion in order to produce high-thrust, highly efficient deep space propulsion systems. The probability of an event such as fusion ignition depends on the number and energies of the positrons interacting with deuteron, which could be increased by increasing the number of beams depositing energized positrons in the D-D implantation volume. Using Geant4 simulations, this study investigates the use of a uniform magnetic field to cluster the positrons resulting from elastic e^+ - e^+ scattering as a means of accumulating independent positron sources for multiple and separate beam generation. Using a combined analysis of cluster size and spread, optimal clustering efficiency was determined to be achievable when the magnetic field strength is at least 0.025 mT for every MeV of energy possessed by the scattered positrons. A potential upper bound on this value of 0.175 mT/MeV was also obtained. In addition to demonstrating this technology's immense potential for enhancing fusion ignition by annihilation, this study also opens a variety of grounds for new research, including the potential of scattering antimatter, the effects of various magnetic field configurations on clustering efficiency, and the ability to produce a large number of particle beams from a mere few scattering on each other.

Introduction

New technologies involving the use of antimatter for advanced space propulsion aim to excite high-energy fusion with beams of antiparticles, namely positrons.[10] The probability of ignition in the fusion material is highly dependent on the energy and densities of the beam packets.[10] This study is largely based on the concept of increasing the probability of ignition by increasing number of antiparticles in the implantation volume of the fusion material with the use of multiple beams. In particular, this research focuses on novel means of independent particle accumulation to generate multiple particle beams from only a few initial sources.

Elastic particle-particle scattering can enable independent beam production by diversifying source particle trajectories and allowing for accumulation in different places within a volume. Furthermore, applying a specific configuration of a magnetic field within that volume has the potential to focus those scattered particles into specific section of the volume where they could be accumulated and processed independently to generate a number of particle beams.

This study uses Geant4 simulations primarily to demonstrate the ability of a uniform magnetic field to focus and cluster scattered positrons in multiple and specific regions in space. Given this uniform field, this study also addresses how the magnitude of the magnetic field must compare to the energies of the scattered positrons in order to maximize clustering efficiency.

Background

Antimatter appeals to researchers as a potential energy source for interplanetary/deep space travel because of its incredibly high specific energy/energy density when it annihilates with matter, which is orders of magnitude greater than other known energy processes (chemical, nuclear, electric, solar) at around 90 MJ/μg.[10] Some challenges in developing antimatter propulsion systems have included producing antimatter, moderating antiparticles to usable energies, and trapping/storing antimatter.[10]

Proposed designs using antimatter are predicted to be capable of reaching Mars in 45 days (instead of 8 months) or the nearest star in 40 years (instead of 30,000 years), travelling at

0.1c on picograms of antimatter (Positron Dynamics).

Radioisotope Positron Propulsion

Positrons are around 2000 times easier to produce than antiprotons[10] and are therefore intriguing particles for antimatter propulsion in space. Radioisotope positron propulsion (RPP) uses fast, high-energy positrons produced from naturally decaying radioisotopes, moderates them to lower energies to magnetically trap, accumulate, and condense them into a beam, then uses that beam to annihilate electrons in a fusion material, catalyzing nuclear fusion. That nuclear fusion produces ions which are then magnetically accelerated to produce thrust.[10]

Certain radioisotopes (including but not limited to ^{11}C, ^{13}N, ^{40}K, ^{15}O, ^{26}Al, ^{22}Na, ^{18}F, ^{83}Sr, ^{124}I, ^{79}Kr, ^{58}Co) emit positrons through a process called β^+ decay, which occurs when an up quark changes into a down quark. In this process, which can occur naturally or can be induced by electron capture (or even galactic cosmic rays, for some isotopes), the nucleus of the radioisotope emits a positron, a neutrino, and gamma rays. Because β^+ decay occurs naturally in these isotopes, they are ideal for in-space positron production, because the isotope can seemingly "store" the antimatter within itself. [10]

Positron Moderation

The "hot" positrons that are emitted from beta-plus decaying radioisotopes are travelling at relativistic speeds and must be "slowed/cooled" (moderated) from MeV and keV of energy to a few eV in order to be magnetically trapped. These trapped positrons are then accumulated and fired as low-energy positron beams that will then annihilate with a D-D fusion material, catalyzing the fusion process and producing ions that are then magnetically fired at the rear of the spacecraft to provide thrust.[10]

Positron-Positron Scattering

Because positrons share many properties with electrons (differing only in charge and spin), the fundamental components of electron-electron (Møller) scattering can be applied to positron-positron scattering (Griffiths). Electrons and positrons, sharing a mass of 0.511 MeV,

also share a propagation factor (Griffiths 244) and, by nature, the amplitude and thus cross section for Møller scattering are the same as those calculable for positron-positron scattering (Griffiths).

$$\frac{i\left(\gamma^{\mu} q_{\mu} + mc\right)}{q^{2} - m^{2}c^{2}}$$

(a)

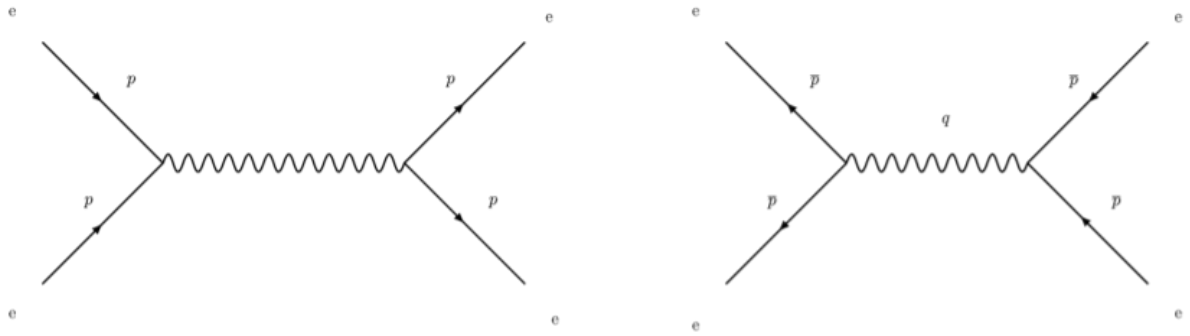

(b) (c)

FIG. 1. (a) The amplitudes for quantum interactions involving either electrons or positrons share this propagation factor. (b) A Feynman diagram depicting one possible interaction in e^- - e^- scattering (c) A Feynman diagram depicting one possible interaction in e^+ - e^+ scattering. Because of the similarities between electrons and positrons, e^+ - e^+ scattering would also likely bear many similarities to e^- - e^- (Møller) scattering.

Method

As Geant4, without additional software, does not allow analysis of beam-beam interactions of primary particle sources, the primary generator component of the software generated 500 random momentum vectors from the center of the volume (0,0,0) for a single run.

The uniform magnetic field in the volume space was designed to align moving charges along the line formed by the points (1,1,1) and (-1,-1,-1). The magnitude of this field was numerically equivalent to the energy of the particle, multiplied by a ratio of the magnetic field

strength *B* to the particle energy *E*. For a specific particle energy, this ratio (B/E) varied from 1e-7 T/MeV to 0.02 T/MeV with an interval of 1e-4 T/MeV to determine what B/E ratio was required to cluster a given run of scattered positrons most effectively. This was repeated for particle energies exclusively ranging from 1 MeV to 50 MeV to analyze how this optimal B/E ratio varied with the e+ energy.

Defining Clusters and Clustering Efficiency

A "cluster" of positrons was defined as the distribution of positrons that had postStepPoint position magnitude between 450 un. and 750 un. Previous runs demonstrated that this was a simple and effective means of isolating and analyzing positrons that were clustered along the line formed by the points (1,1,1) and (-1,-1,-1).

Parameters for determining clustering efficiency were dependent on cluster size (the number of positrons in that cluster) and spread (the standard deviation of the cluster). By definition, an efficiently clustered distribution of scattered positrons would be highly populated and highly concentrated, having a large cluster size and small standard deviation. Therefore, a ratio of these two values (cluster size *n* divided by standard deviation *sd*), as plotted for a range of B/E ratios for a single positron energy, would display a peak *n*/*sd* for the B/E ratio that most effectively clusters the scattered positrons. That B/E ratio would be considered optimal B/E ratio for clustering scattered positrons with energy *E*.

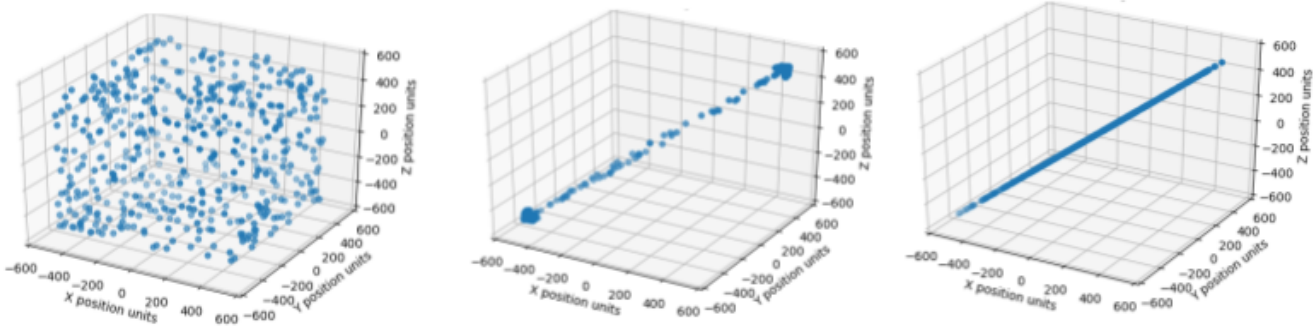

(a) (b) (c)

FIG. 2. The effect of varying the magnetic field strength on the clustering of the scattered positrons. (a) B/E = 0 mT/MeV (b) B/E = 0.099 mT/MeV (c) B/E = 20 mT/MeV

The 3D plots in Figure 2 depict that effect of using the optimal B/E ratio to cluster the scattered positrons. Positrons that are pushed by the uniform magnetic field have a tendency to align themselves along a line running from opposing corners of the volume space, as designed. Analysis of these clusters will refer to the cluster in the all-positive sector of the volume space as the “right cluster” and the cluster in the all-negative sector of the volume space as the “left cluster”.

When the ratio of the magnitude of the magnetic field to the energy of the particles is less than optimal B/E ratio for that specific particle energy (a), the positrons are not clustered at all, and their final positions remain scattered and unfocused. When the ratio of the magnitude of the magnetic field to the energy of the particles is greater than optimal B/E ratio for that specific particle energy (c), the final positions of the scattered positrons in the uniform field seems to distribute themselves evenly along line formed by the points (1,1,1) and (-1,-1,-1), which disallows them to settle within the defined cluster bounds.

However, when the ratio of the magnitude of the magnetic field to the energy of the particles is approximately equal to the optimal B/E ratio (b), the cluster of positrons becomes extremely apparent. The cluster actually takes on a defined arrowhead-like shape, and further analysis of that shape and its significance toward particle positron accumulator design will require more research.

Data

(a)

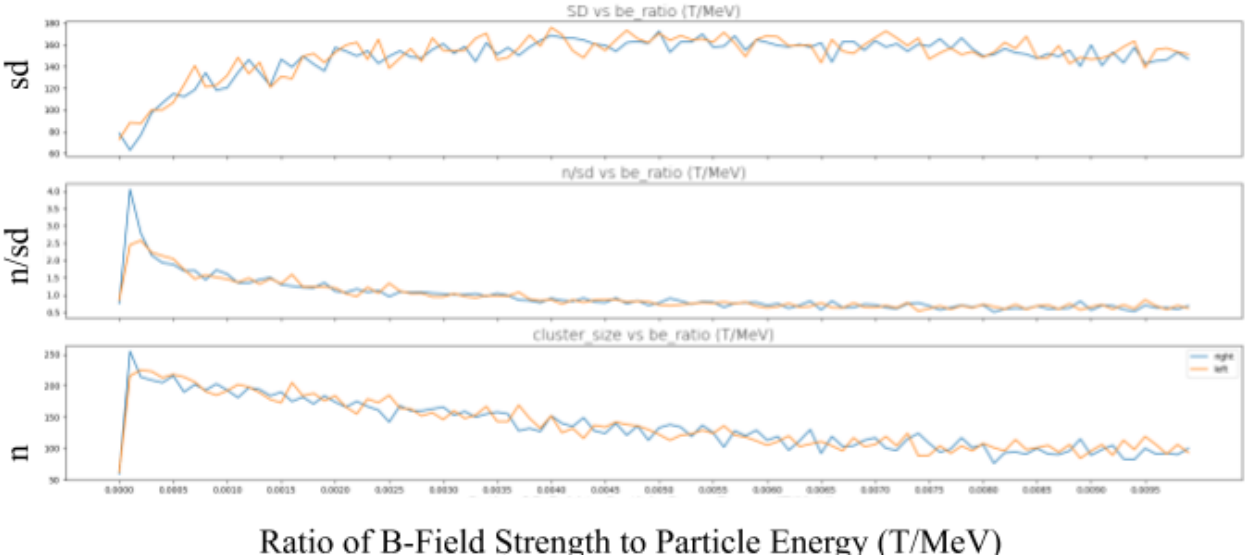

(b)

FIG. 3 B/E ratio's effect on clustering efficiency parameters at specific particle energies. The orange line represents the parameters of the left cluster (-1,-1,-1); the blue line represents the parameters of the right cluster (1,1,1) (a) E = 9 MeV (b) E = 24 MeV

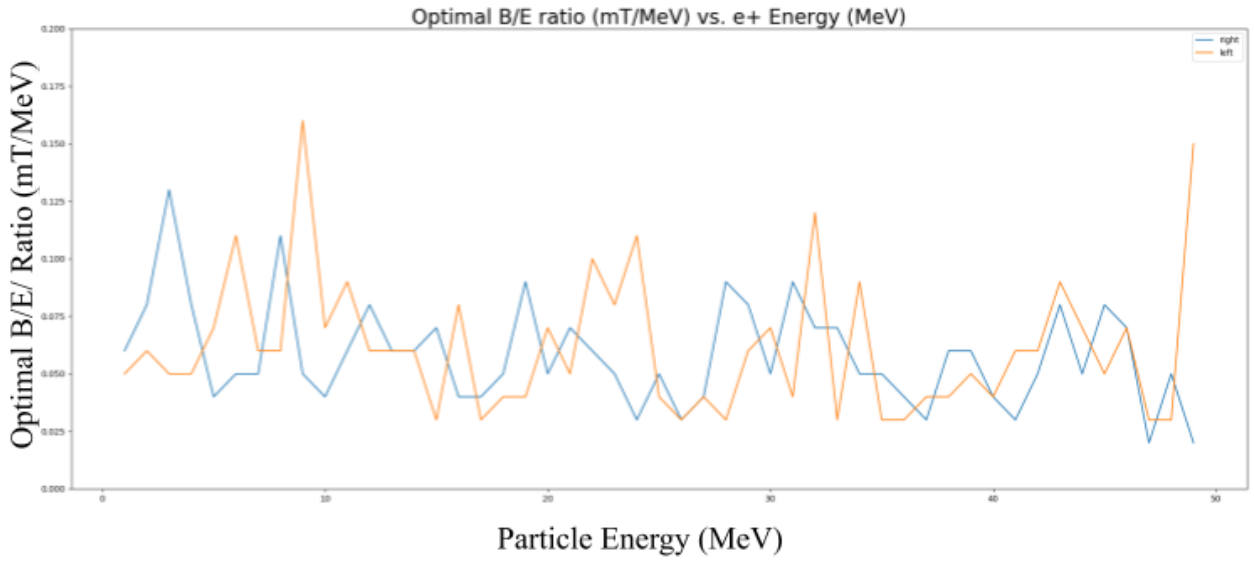

FIG. 4. The optimal B/E ratio for particle energies between 1 MeV and 50 MeV appear to range from 0.025 mT/MeV to 0.175 mT/MeV with no particular preference

Discussion

Varying the B/E Ratio for a Specific E

Figure 3 depicts two example plots of simulations that varied the B/E ratio to observe how parameters of the resulting clusters changed. For a variety of particle energies ranging from 1 MeV to 49 MeV, these plots actually changed very little, and the minor deviations that were present from plot to plot could easily be attributed to the random nature of the Geant4 simulations.

In each plot, the standard deviation of the cluster (*sd*) decreased between 0 T/MeV and the optimal B/E ratio. At approximately the optimal B/E ratio, the standard deviation reached its minimum value for both clusters, as expected. As the B/E ratio increased, however, the standard deviation of the cluster increased dramatically as well.

The cluster size (*n*) increased dramatically between 0 T/MeV and the optimal B/E ratio. At approximately the optimal ratio, the left and right cluster sizes were at their peaks, as

expected. In fact, each cluster size peaked relatively close to a count of 250 positrons, which is half of the total number of positrons scattered in the volume (500), suggesting that at that optimal B/E ratio, the magnetic field had the proper magnitude to effectively cluster nearly all of the scattered positrons.

Finally, ratio of the size *n* to the standard deviation *sd* also increased dramatically between 0 T/MeV and the optimal B/E ratio, then decreased as B/E ratio increased. At approximately the optimal B/E ratio, *n/sd* peaked, demonstrating that the B/E ratio altered the magnetic field strength in that specific run most effectively clustered the scattered positrons.

This suggests that as the B/E ratio approaches the optimal value from the left, the concentration of the positrons within 450 un. and 700 un. away from the origin increases. After this optimal ratio, the magnetic field increases in strength and the number of positrons within those bounds decreases while their overall spread increases, suggesting that magnetic fields stronger than the optimal strength designated by the optimal B/E ratio may not be as well suited to cluster the scattered positrons within 450 un. and 700 un. away from the origin along the (±1,±1,±1) spatial vector.

Bounds on B/E Ratio

For each particle energy E, the B/E ratio that caused *n/sd* to peak as seen in Figure 3 was recorded and plotted against E. As seen in Figure 4, the optimal B/E for positrons with any energy between 1 MeV and 50 MeV can be placed between 0.025 mT/MeV and 0.175 mT/MeV. The uncertainty of this specific value is also an artifact of the randomness of the Geant4 simulations. As no discernable trend from Figure 4 can describe the variation of the optimal B/E as the particle energy increases, this range is an acceptable means of calculating the necessary strength of the magnetic field required to efficiently cluster beam-beam scattered positrons.

Interpreting postStepPoint

The positions of the positrons as recorded by the Geant4 G4Step's postStepPoint three-vector were used for the described clustering efficiency analysis. Some ambiguities, however, in this analysis arise.

For example, if the postStepPoint is the particle's final position at the end of the run (in essence, where the particle "stops"), then the optimal B/E is between 0.025 mT/MeV and 0.175 mT/MeV.

If the postStepPoint is the particle's final position at the end of the step (implying that the particles continues moving in that direction), then the optimal B/E ratios are above the minimum B/E (0.025 mT/MeV). The resulting cluster should only become more focused as the magnetic field increases in strength, since the particles that were recorded before reaching the 450 un. lower bound of the cluster would continue along their altered trajectory and any accumulator within the cluster bounds, even if the particle didn't actually settle within those bounds by the end of the run.

Regardless, the B/E ratio that results in optimal clustering efficiency is above 0.025 mT/MeV, and investigation into the nuances of that threshold and its significance toward positron accumulator design are grounds for upcoming phases of this research.

Conclusion

This study demonstrates the ability of a uniform magnetic field to efficiently cluster scattered positrons. The most effective magnetic fields have strengths of at least 0.025 mT for every MeV of energy possessed by the scattered positrons, with a potential upper bound of 0.175 mT/MeV. This demonstration of effective clustering allows for the efficient design and placement of particle accumulators that can receive those clustered postitrons, independently focusing them into beams that, when directed at the same implantation volume of a D-D fusion material, will increase the probability of ignition.

Next Steps

Short-term continuation of this research is directed towards investigating other magnetic field configurations, seeking to diversify scattered trajectories further and produce more clusters. Long-term continuation seeks to design efficient accumulators for trapping and bunching the clustered positrons into beams that can be pulsed towards a D-D fusion material.

References:

1. Beling, C. D., Simpson, R. I., Charlton, M., Jacobsen, F. M., Griffith, T. C., Moriarty, P., & Fung, S. (1987). A field-assisted moderator for low-energy positron beams. Applied Physics A Solids and Surfaces, 42(2), 111–116.doi:10.1007/bf00616719
2. Dunbar, B. (n.d.). New and Improved Antimatter Spaceship for Mars Missions. Retrieved from https://www.nasa.gov/centers/goddard/news/topstory/2006/antimatter_spaceship.html
3. Epstein, C.S., Johnston, R., Lee, S., Bernauer, J.C., Corliss, R.C., Dow, K., Fisher, P., Friščić, I., Hasell, D., Milner, R.G., Moran, P., Steadman, S.G., Dodge, J., Ihloff, E., Kelsey, J., Vidal, C., & Cooke, C.M. (2019). Measurement of Moller Scattering at 2.5 MeV.
4. Greaves, R. ., Gilbert, S. ., & Surko, C. . (2002). Trap-based positron beams. Applied Surface Science, 194(1-4), 56–60. doi:10.1016/s0169-4332(02)00089-2
5. Griffiths, D. J. (2014). Introduction to elementary particles. Weinheim: Wiley-VCH Verlag.
6. Hall, L. (2018, March 28). Radioisotope Positron Propulsion. Retrieved from https://www.nasa.gov/directorates/spacetech/niac/2018_Phase_I_Phase_II/Radioisotope_Positron_Propulsion/
7. Hamdi, H., Salje, E. K. H., Ghosez, P., & Bousquet, E. (2016). First-principles reinvestigation of bulk WO3. Physical Review B, 94(24).doi:10.1103/physrevb.94.245124
8. Lynn, K.G. & McKee, B.T.A. Appl. Phys. (1979) 19: 247. https://doi.org/10.1007/BF00900467
9. Merrison, J. P., Charlton, M., Deutch, B. I., & Jorgensen, L. V. (1992). Field assisted positron moderation by surface charging of rare gas solids. Journal of Physics: Condensed Matter,4(12). doi:10.1088/0953-8984/4/12/003
10. Weed, R., PhD, Machacek, J., Phd, & Ramamurthy, B. (n.d.). Radioisotope Positron Propulsion: NIAC Phase I Report (Rep.). Retrieved June 11, 2019, from https://ntrs.nasa.gov/archive/nasa/casi.ntrs.nasa.gov/20190018063.pdf.

11. Williams, A. I., Murtagh, D. J., Fayer, S. E., Andersen, S. L., Chevallier, J., Kövér, Á., … Laricchia, G. (2015). Moderation and diffusion of positrons in tungsten meshes and foils. Journal of Applied Physics, 118(10), 105302. doi:10.1063/1.4930033